Search for triaxially deformed halo nucl

Jie MENG （孟 杰）
School of Physics，Peking University（北京大学物理学院）

(Time-depend) CDFT in 3D lattice

EoM on 3D lattice with the inverse Hamiltonian and Fourier spectral methods.

Linear 3α clusters chain structure for ^{12}C against the bending and fission in **cranking CDFT** and **TD CDFT** on a 3D lattice

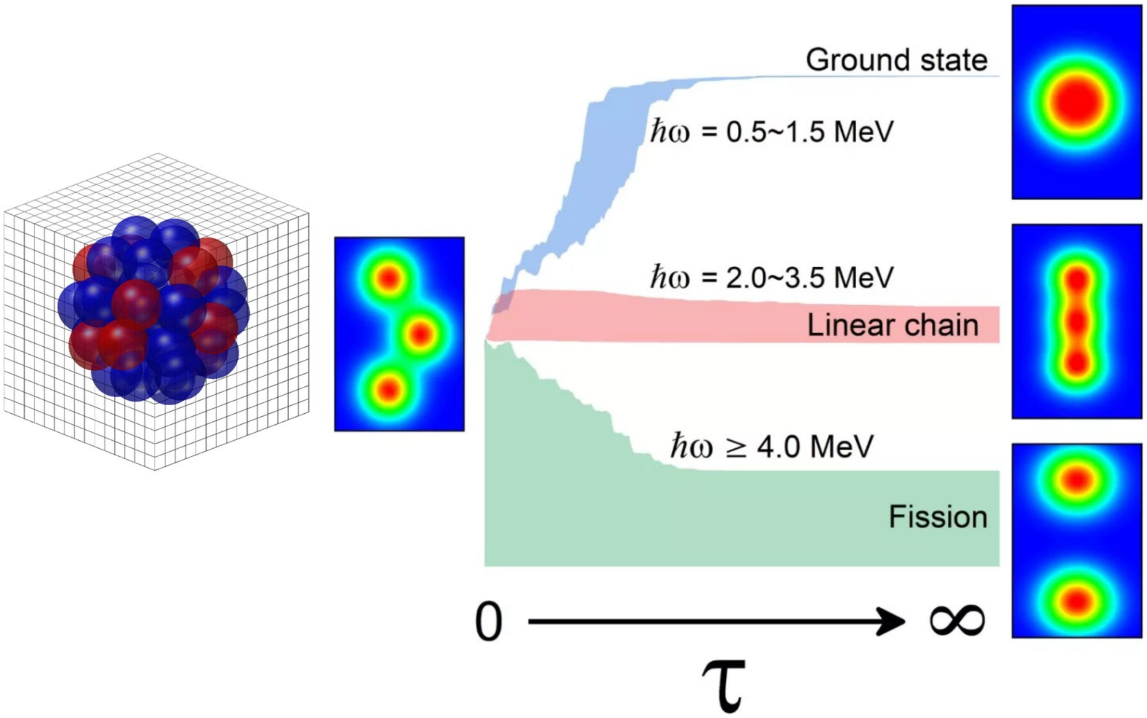

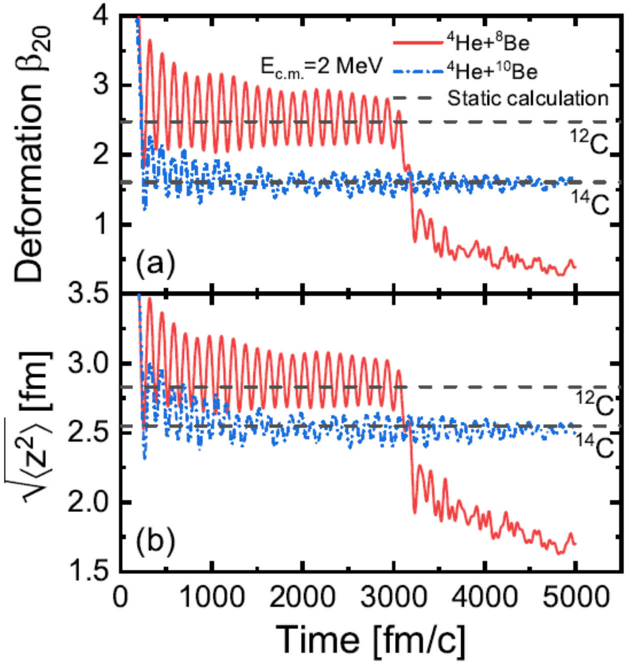

Ren, Zhang, Zhao, Itagaki, Maruhn, Meng, SCPMA 62, 112062 (2019)
Ren, Zhao, Meng, Physics Letters B 801 (2020) 135194

Toroidal states in ^{28}Si

7α disassembly of ^{28}Si

Cao et al., Phys. Rev. C 99, 014606 (2019)

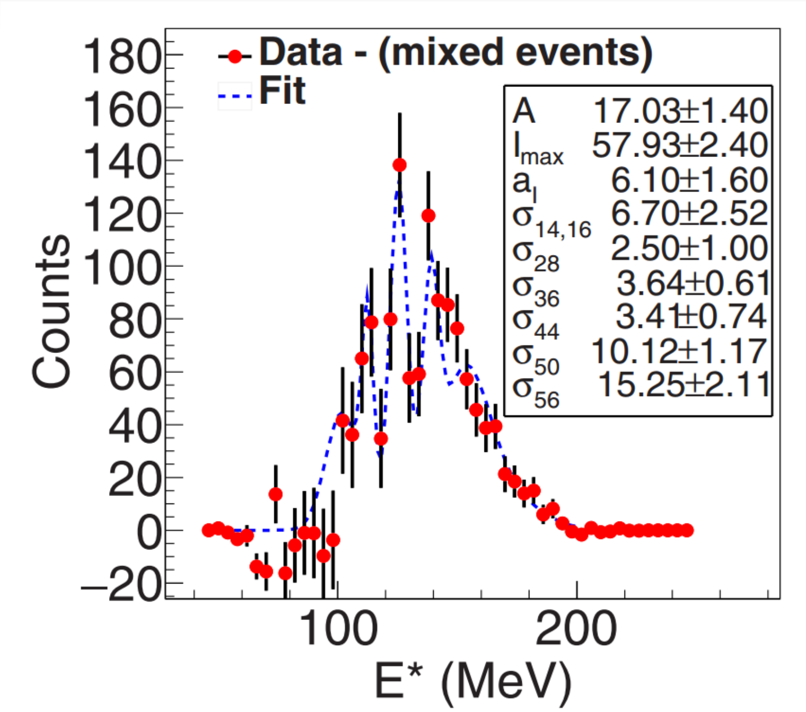

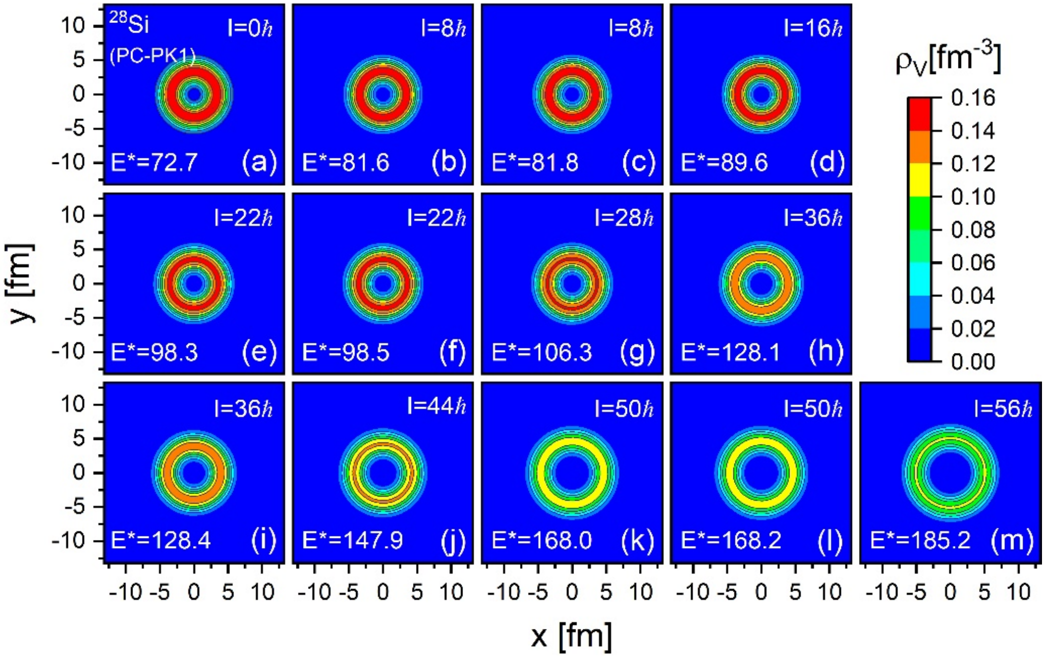

Density distributions in the z = 0 plane for the toroidal states in cranking CDFT on a 3D lattice

Ren, Zhao, Zhang, Meng, Nuclear Physics A996 (2020) 121696

(Time-depend) CDFT in 3D lattice

PHYSICAL REVIEW LETTERS **128,** 172501 (2022)

Dynamical Synthesis of ^{4}He in the Scission Phase of Nuclear Fission

Z. X. Ren,[1] D. Vretenar,[2,1,*] T. Nikšić,[2,1] P. W. Zhao,[1,†] J. Zhao,[3] and J. Meng[1,‡]

[1]*State Key Laboratory of Nuclear Physics and Technology, School of Physics, Peking University, Beijing 100871, China*
[2]*Physics Department, Faculty of Science, University of Zagreb, 10000 Zagreb, Croatia*
[3]*Center for Circuits and Systems, Peng Cheng Laboratory, Shenzhen 518055, China*

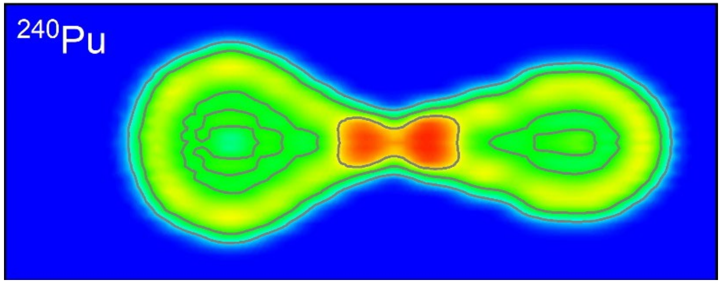

裂变原子核在断裂点附
近的局域化函数分布

- Z. X. Ren, J. Zhao, D. Vretenar, T. Nikšić, P. W. Zhao, and J. Meng, Microscopic analysis of induced nuclear fission dynamics, **Phys. Rev. C** 105, 044313 (2022)
- Z. X. Ren, D. Vretenar, T. Nikšić, P. W. Zhao, J. Zhao, and J. Meng, Dynamical synthesis of ^{4}He in the scission phase of nuclear fission, **Phys. Rev. Lett.** 128, 172501 (2022)

(Time-depend) CDFT in 3D lattice

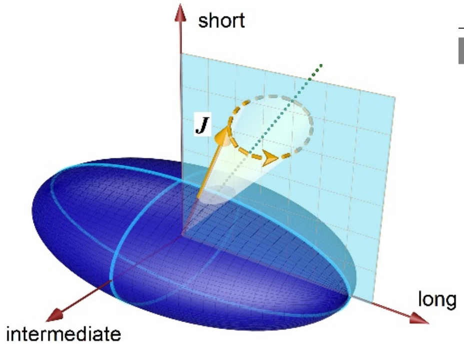

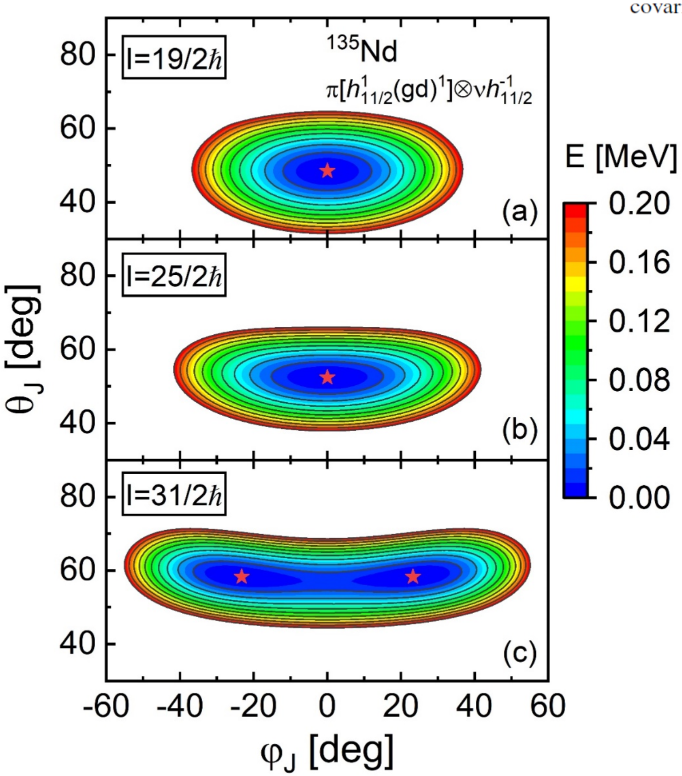

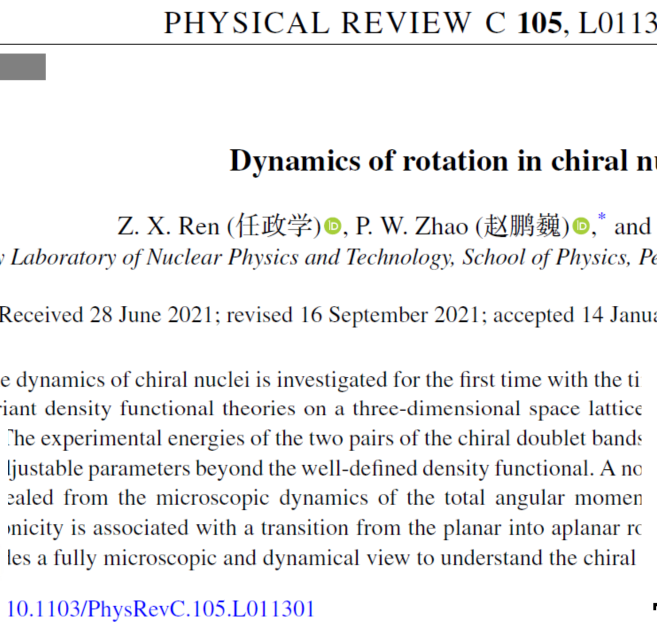

PHYSICAL REVIEW C **105**, L011301 (2022)

Letter

Dynamics of rotation in chiral nuclei

Z. X. Ren (任政学), P. W. Zhao (赵鹏巍),* and J. Meng (孟杰)†

State Key Laboratory of Nuclear Physics and Technology, School of Physics, Peking University, Beijing 100871, China

(Received 28 June 2021; revised 16 September 2021; accepted 14 January 2022; published 31 January 2022)

The dynamics of chiral nuclei is investigated for the first time with the ti
covariant density functional theories on a three-dimensional space lattice
he experimental energies of the two pairs of the chiral doublet bands
ljustable parameters beyond the well-defined density functional. A no
ealed from the microscopic dynamics of the total angular momen
nicity is associated with a transition from the planar into aplanar rc
les a fully microscopic and dynamical view to understand the chiral

10.1103/PhysRevC.105.L011301

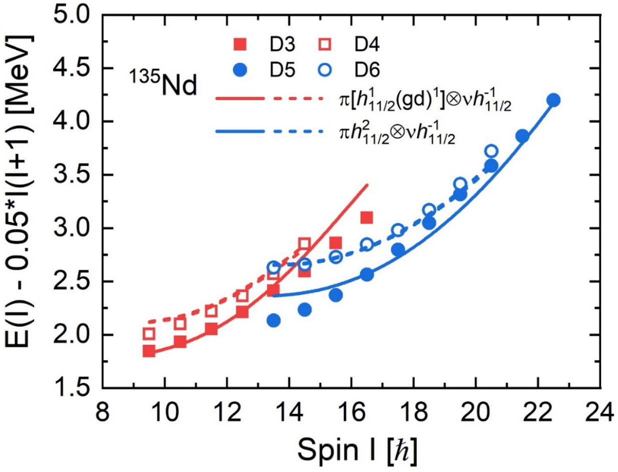

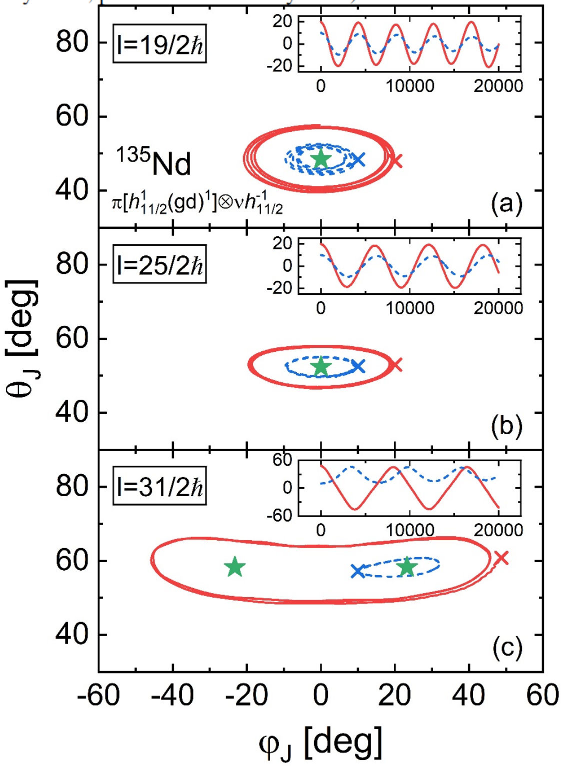

ELSEVIER
journal homepage: www.elsevier.com/locate/scib
www.scibull.c

Article

Selection rules of electromagnetic transitions for chirality-parity violation in atomic nuclei

Yuanyuan Wang [a], Xinhui Wu [a], Shuangquan Zhang [a,*], Pengwei Zhao [a], Jie Meng [a,b,c]

[a] State Key Laboratory of Nuclear Physics and Technology, School of Physics, Peking University, Beijing 100871, China
[b] School of Physics and Nuclear Energy Engineering, Beihang University, Beijing 100191, China
[c] Yukawa Institute for Theoretical Physics, Kyoto University, Kyoto 606-8502, Japan

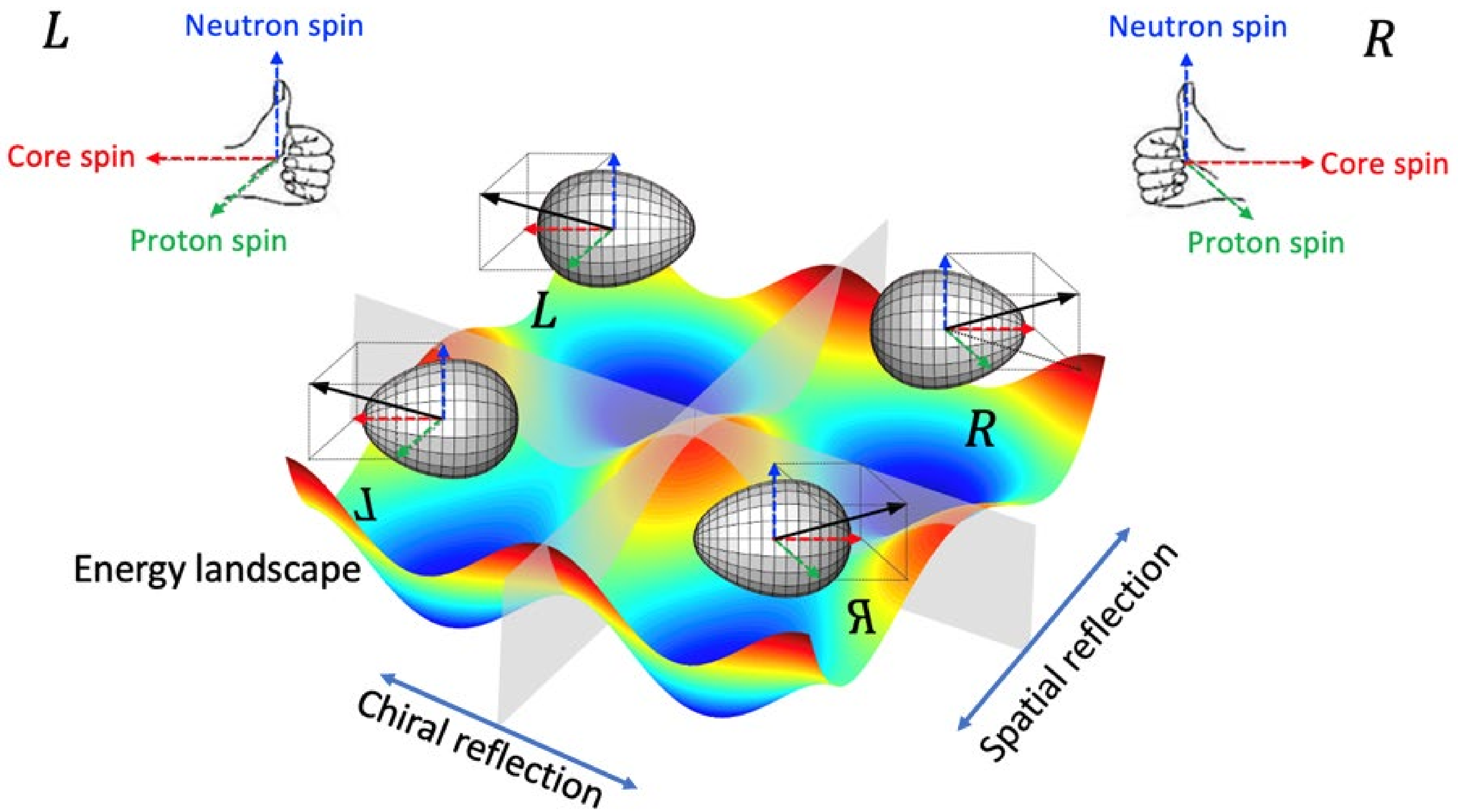

Nuclear Chirality-Parity (ChP) violation

ab initio calculation

Relativistic Brueckner Hartree-Fock Theory

Shi-Hang Shen, Jin-Niu Hu,Hao-Zhao Liang, Jie Meng, Peter Ring, Shuang-Quan Zhang,
Relativistic Brueckner–Hartree–Fock Theory for Finite Nuclei .

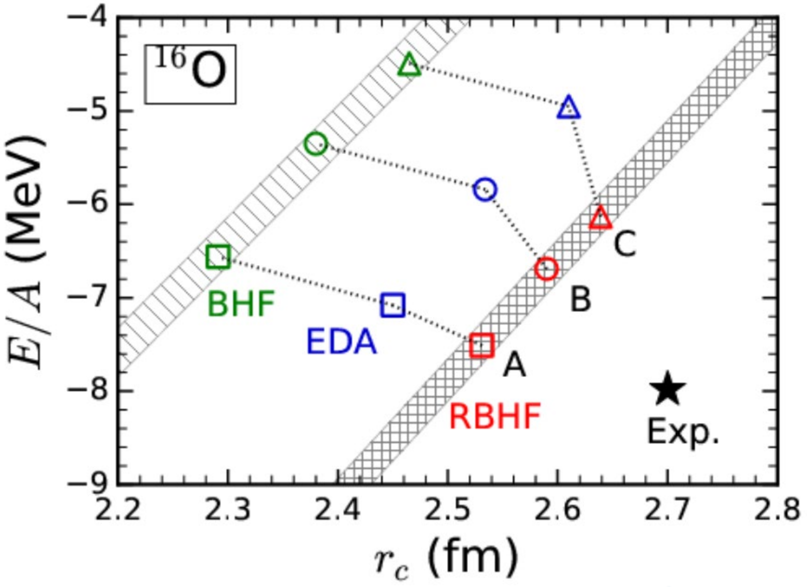

Energies and charge radii of ^{16}O in RBHF in comparison with EDA and BHF

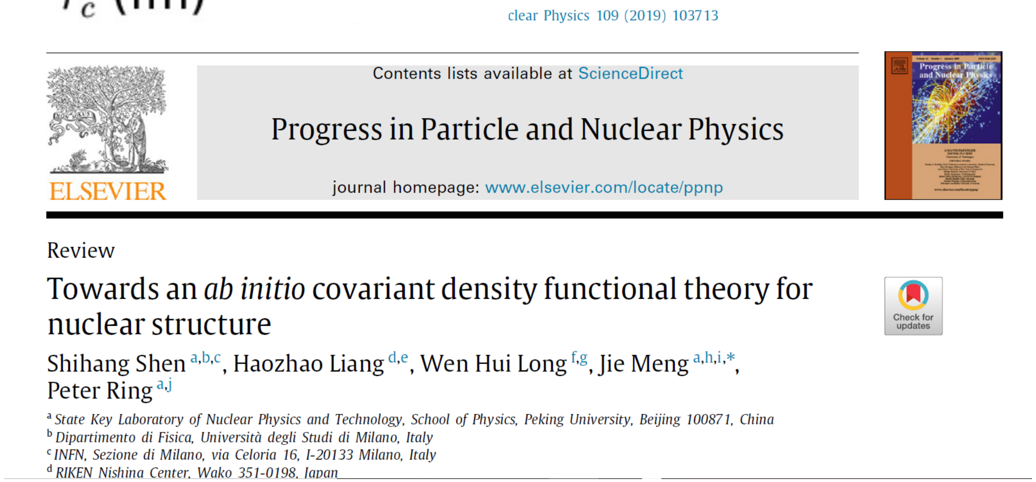

clear Physics 109 (2019) 103713

Contents lists available at ScienceDirect

Progress in Particle and Nuclear Physics

journal homepage: www.elsevier.com/locate/ppnp

Review

Towards an *ab initio* covariant density functional theory for nuclear structure

Shihang Shen[a,b,c], Haozhao Liang[d,e], Wen Hui Long[f,g], Jie Meng[a,h,i,*], Peter Ring[a,j]

[a] State Key Laboratory of Nuclear Physics and Technology, School of Physics, Peking University, Beijing 100871, China
[b] Dipartimento di Fisica, Università degli Studi di Milano, Italy
[c] INFN, Sezione di Milano, via Celoria 16, I-20133 Milano, Italy
[d] RIKEN Nishina Center, Wako 351-0198, Japan

Tensor effects on spin-Orbit Splitting

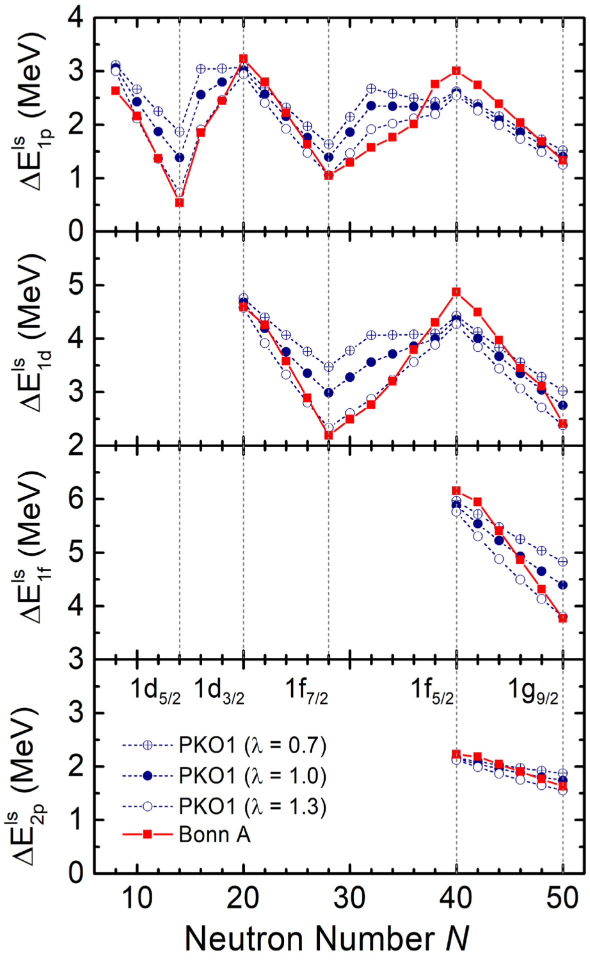

- **Neutron drop is a neutron system confined in an external field.**

……

- **A neutron drop provides also an ideal and simple system to investigate the effects of tensor forces.**

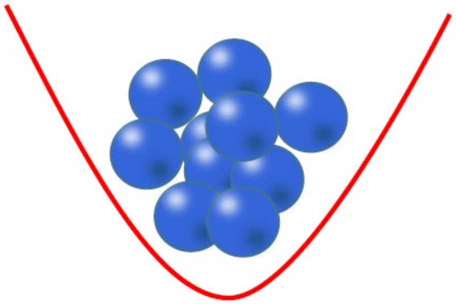

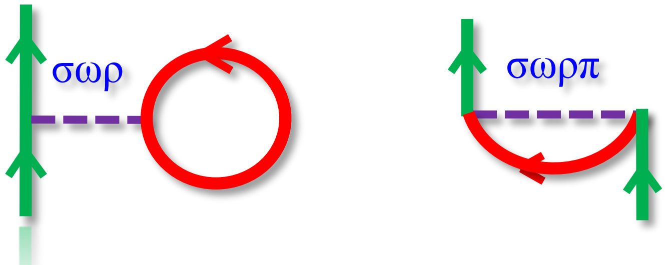

Shi-Hang Shen, Hao-Zhao Liang, Jie Meng, Peter Ring, Shuang-Quan Zhang,
Effects of tensor forces in nuclear spin–orbit splittings from ab initio calculations.
Phys. Lett. B778 (2018) 344–348
Relativistic Brueckner-Hartree-Fock theory for neutron drops
Phys. Rev. C 97, 054312 (2018)

- **RHF** shows similar pattern, mainly contributed by ***π*NN tensor interaction**.
- Neither RBHF nor CDFT includes **beyond-mean-field effects** → **a fair comparison!**

ab initio calculation

Relativistic Brueckner Hartree-Fock Theory

PHYSICAL REVIEW C **98**, 054302 (2018)

Relativistic Brueckner-Hartree-Fock theory in nuclear matter without the average momentum approximation

Hui Tong (童辉),[1] Xiu-Lei Ren (任修磊),[1,2] Peter Ring,[1,3] Shi-Hang Shen (申时行),[1]
Si-Bo Wang (王锶博),[1] and Jie Meng (孟杰)[1,4,5,*]
[1] *State Key Laboratory of Nuclear Physics and Technology, School of Physics, Peking University, Beijing 100871, C*
[2] *Institut für Theoretische Physik II, Ruhr-Universität Bochum, D-44780 Bochum, Germany*
[3] *Physik-Department der Technischen Universität München, D-85748 Garching, Germany*
[4] *Department of Physics, University of Stellenbosch, Stellenbosch, South Africa*

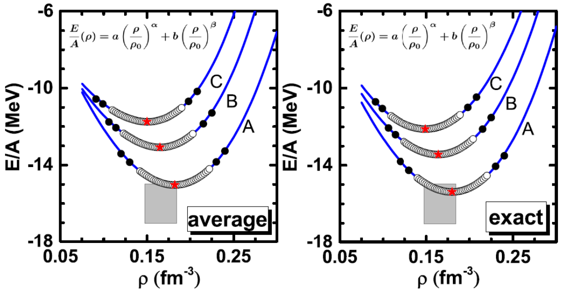

FIG. 1. Binding energy per nucleon for nuclear matter as a function of the total density ρ. Results for Bonn potentials A, B, C with (left panel) and without (right panel) c.m. momentum approximation are shown. The RBHF results are represented by open and solid circles, where open circles stand for the data used in the fit and solid circles indicate the validity of the results of the fit (solid curves). The red stars indicate the saturation points obtained from RBHF results.

PHYSICAL REVIEW C **103**, 054319 (2021)

Nuclear matter in relativistic Brueckner-Hartree-Fock theory with Bonn potential in the full Dirac space

Sibo Wang,[1] Qiang Zhao,[1] Peter Ring,[1,2] and Jie Meng[1,3,*]
[1] *State Key Laboratory of Nuclear Physics and Technology, School of Physics, Peking University, Beijing 100871, China*
[2] *Department of Physik, Technische Universität München, D-85747 Garching, Germany*
[3] *Yukawa Institute for Theoretical Physics, Kyoto University, Kyoto 606-8502, Japan*

(Received 25 March 2021; accepted 11 May 2021; published 24 May 2021)

Starting from the Bonn potential, the relativistic Brueckner-Hartree-Fock (RBHF) equations are solved for nuclear matter in the full Dirac space, which provides a unique way to determine the single-particle potentials and avoids the approximations applied in the RBHF calculations in the Dirac space with positive-energy states (PESs) only. The uncertainties of the RBHF calculations in the Dirac space with PESs only are investigated, and the importance of RBHF calculations in the full Dirac space is demonstrated. In the RBHF calculations in the full Dirac space, the empirical saturation properties of symmetric nuclear matter are reproduced, and the obtained equation of state agrees with the results based on the relativistic Green's function approach up to the saturation density.

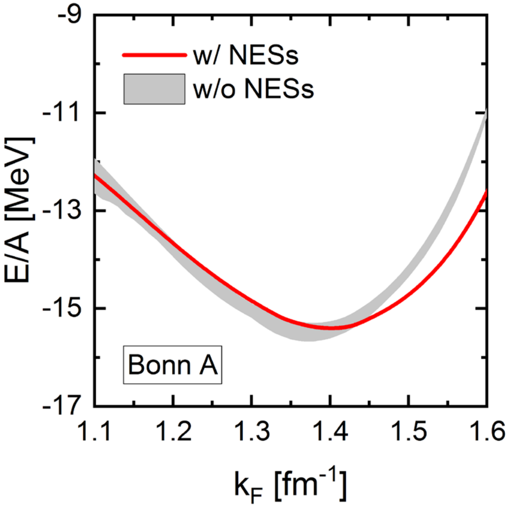

Relativistic NN interaction

□ Chiral Nucleon-Nucleon Interaction

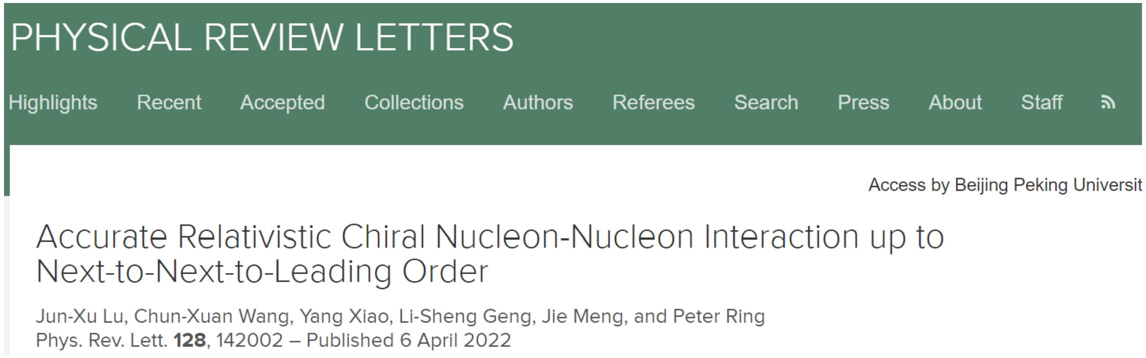

PHYSICAL REVIEW LETTERS

Highlights Recent Accepted Collections Authors Referees Search Press About Staff

Access by Beijing Peking Universit

Accurate Relativistic Chiral Nucleon-Nucleon Interaction up to Next-to-Next-to-Leading Order

Jun-Xu Lu, Chun-Xuan Wang, Yang Xiao, Li-Sheng Geng, Jie Meng, and Peter Ring

Phys. Rev. Lett. **128**, 142002 – Published 6 April 2022

X. L. Ren, K. W. Li, L. S. Geng, B. W. Long, P. Ring, and J. Meng,

Leading order relativistic chiral nucleon-nucleon interaction,

Chin. Phys. C 42, 014103(2018) J

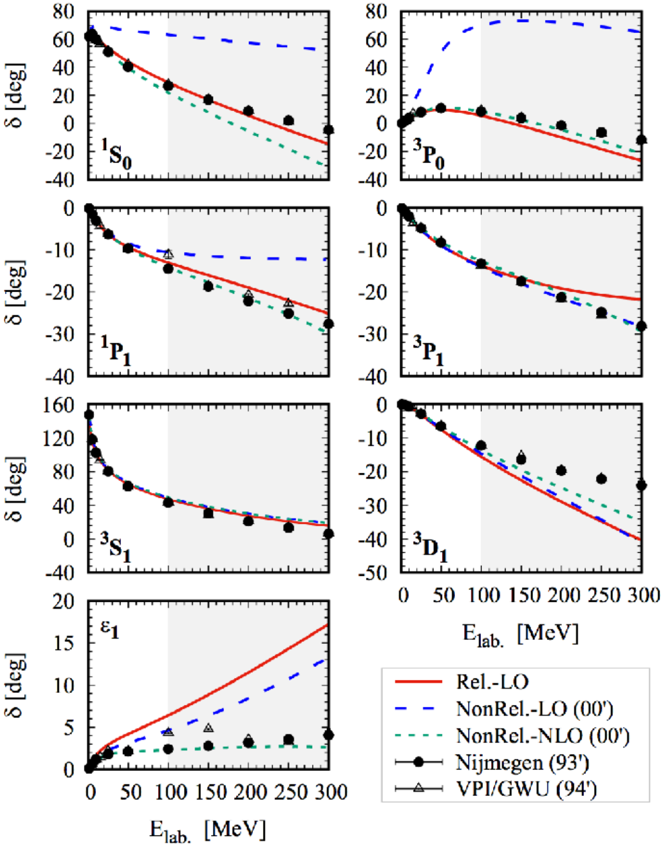

□ Baryon Interaction by lattice QCD

PHYSICAL REVIEW LETTERS

Highlights Recent Accepted Collections Authors Referees Search Press About Staff

Accepted Paper

Dibaryon with highest charm number near unitarity from lattice QCD

Phys. Rev. Lett.

Yan Lyu, Hui Tong, Takuya Sugiura, Sinya Aoki, Takumi Doi, Tetsuo Hatsuda, Jie Meng, and Takaya Miyamoto

Accepted 2 July 2021

High-precision relativistic nucleon force up to NNLO

Density functional from machine learning

$$E[\rho] = T[\rho] + U[\rho] + \int V(\mathbf{r})\rho(\mathbf{r})\,\mathrm{d}^3\mathbf{r}$$

H-K Theorem proves the existence of a universal functional depends solely on density.

BUT, all previous attempts for a nuclear kinetic energy functional FAILS.

→ One has to introduce Kohn-Sham, i.e., a functional of orbits

$$T[\rho] \doteq \sum_{i=1}^{N} \left\langle \varphi_i \left| -\frac{\hbar^2}{2m}\nabla^2 \right| \varphi_i \right\rangle$$

By Machine Learning, a robust and accurate orbital-free density functional is established !

Robust self-consistent solution

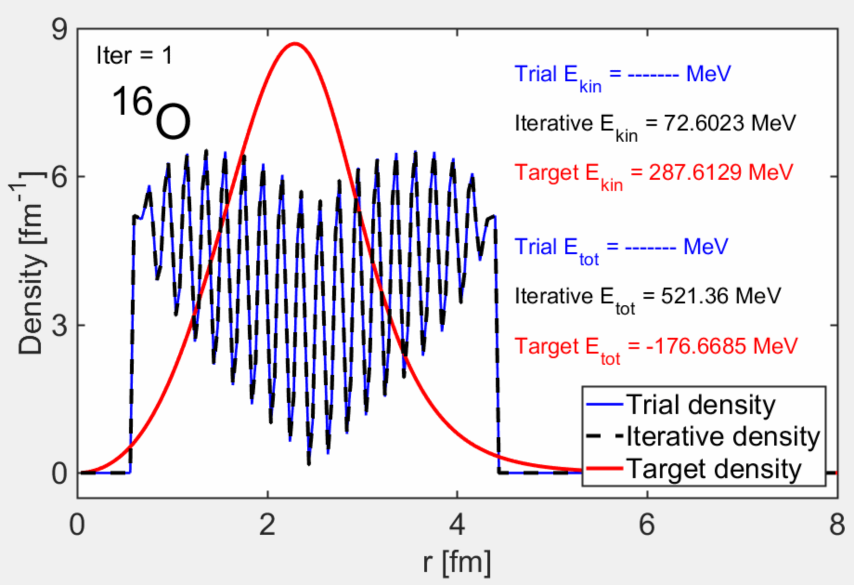

Most accurate ever orbit-free DFT for nuclei

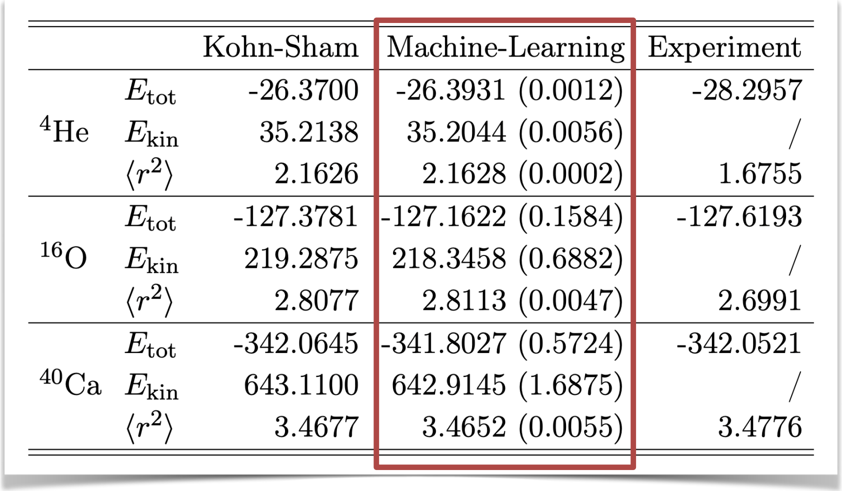

		Kohn-Sham	Machine-Learning	Experiment
^{4}He	$E_{\rm tot}$	-26.3700	-26.3931 (0.0012)	-28.2957
	$E_{\rm kin}$	35.2138	35.2044 (0.0056)	/
	$\langle r^2\rangle$	2.1626	2.1628 (0.0002)	1.6755
^{16}O	$E_{\rm tot}$	-127.3781	-127.1622 (0.1584)	-127.6193
	$E_{\rm kin}$	219.2875	218.3458 (0.6882)	/
	$\langle r^2\rangle$	2.8077	2.8113 (0.0047)	2.6991
^{40}Ca	$E_{\rm tot}$	-342.0645	-341.8027 (0.5724)	-342.0521
	$E_{\rm kin}$	643.1100	642.9145 (1.6875)	/
	$\langle r^2\rangle$	3.4677	3.4652 (0.0055)	3.4776

X. H. Wu, Z. X. Ren, P. W. Zhao, Phys. Rev. C, 105, L031303 (2022)

Outline

- Introduction
- Theoretical framework
- Results and discussion
- Summary

Halo nuclei

- ➢ Halo nuclei have attracted lots of attention since the discovery of the halo phenomenon in ^{11}Li.

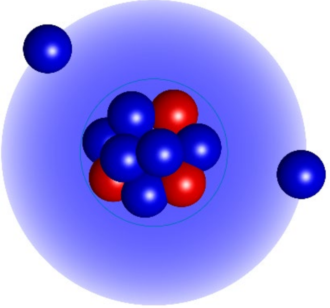

^{11}Li

Tanihata *et al.*, PRL 55, 2676 (1985)
Tanihata *et al.*, PPNP 68, 215 (2013)

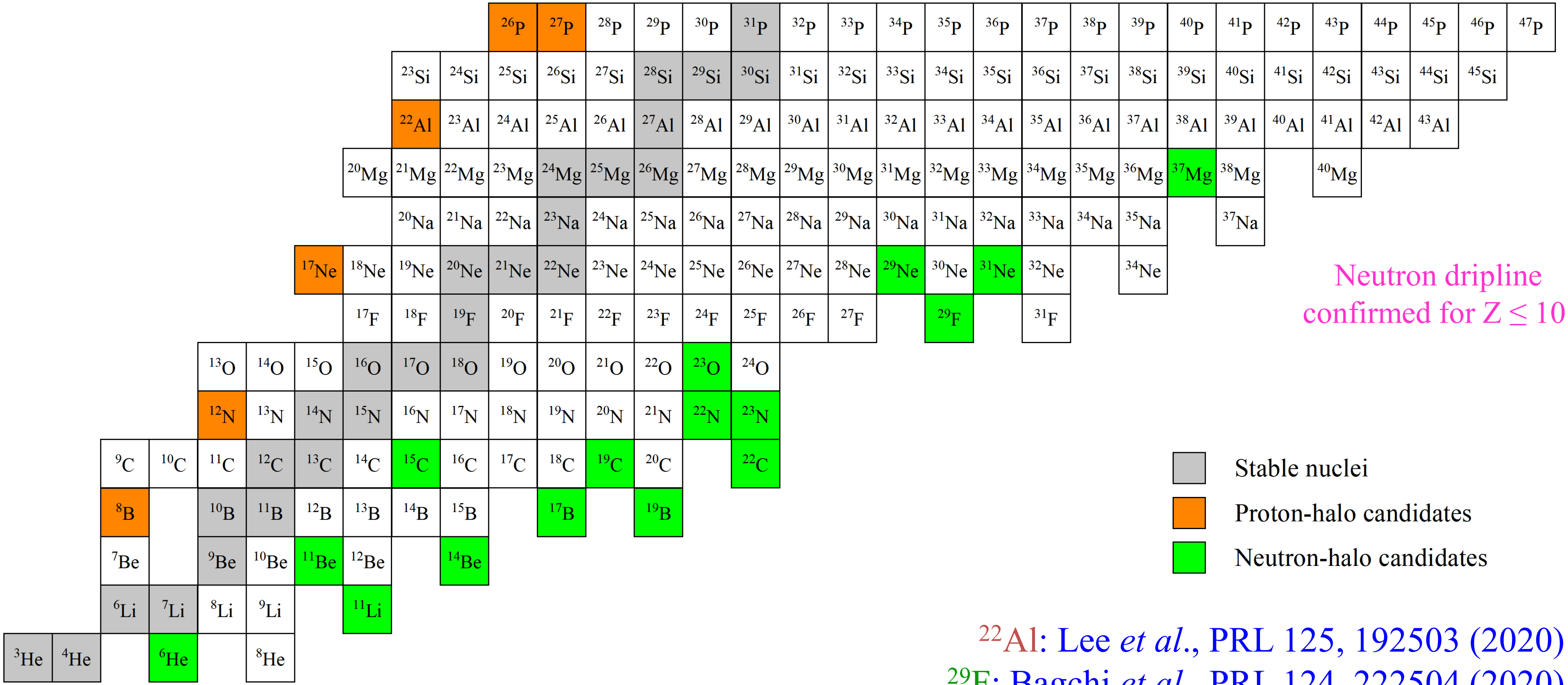

										^{26}P 🟧	^{27}P 🟧	^{28}P	^{29}P	^{30}P	^{31}P ▨	^{32}P	^{33}P	^{34}P	^{35}P	^{36}P	^{37}P	^{38}P	^{39}P	^{40}P	^{41}P	^{42}P	^{43}P	^{44}P	^{45}P	^{46}P	^{47}P
								^{23}Si	^{24}Si	^{25}Si	^{26}Si	^{27}Si	^{28}Si ▨	^{29}Si ▨	^{30}Si ▨	^{31}Si	^{32}Si	^{33}Si	^{34}Si	^{35}Si	^{36}Si	^{37}Si	^{38}Si	^{39}Si	^{40}Si	^{41}Si	^{42}Si	^{43}Si	^{44}Si	^{45}Si	
								^{22}Al 🟧	^{23}Al	^{24}Al	^{25}Al	^{26}Al	^{27}Al ▨	^{28}Al	^{29}Al	^{30}Al	^{31}Al	^{32}Al	^{33}Al	^{34}Al	^{35}Al	^{36}Al	^{37}Al	^{38}Al	^{39}Al	^{40}Al	^{41}Al	^{42}Al	^{43}Al		
							^{20}Mg	^{21}Mg	^{22}Mg	^{23}Mg	^{24}Mg ▨	^{25}Mg ▨	^{26}Mg ▨	^{27}Mg	^{28}Mg	^{29}Mg	^{30}Mg	^{31}Mg	^{32}Mg	^{33}Mg	^{34}Mg	^{35}Mg	^{36}Mg	^{37}Mg 🟩	^{38}Mg		^{40}Mg				
								^{20}Na	^{21}Na	^{22}Na	^{23}Na ▨	^{24}Na	^{25}Na	^{26}Na	^{27}Na	^{28}Na	^{29}Na	^{30}Na	^{31}Na	^{32}Na	^{33}Na	^{34}Na	^{35}Na		^{37}Na						
						^{17}Ne 🟧	^{18}Ne	^{19}Ne	^{20}Ne ▨	^{21}Ne ▨	^{22}Ne ▨	^{23}Ne	^{24}Ne	^{25}Ne	^{26}Ne	^{27}Ne	^{28}Ne	^{29}Ne 🟩	^{30}Ne	^{31}Ne 🟩	^{32}Ne		^{34}Ne								
							^{17}F	^{18}F	^{19}F ▨	^{20}F	^{21}F	^{22}F	^{23}F	^{24}F	^{25}F	^{26}F	^{27}F		^{29}F 🟩		^{31}F										
					^{13}O	^{14}O	^{15}O	^{16}O ▨	^{17}O ▨	^{18}O ▨	^{19}O	^{20}O	^{21}O	^{22}O	^{23}O 🟩	^{24}O															
					^{12}N 🟧	^{13}N	^{14}N ▨	^{15}N ▨	^{16}N	^{17}N	^{18}N	^{19}N	^{20}N	^{21}N	^{22}N 🟩	^{23}N 🟩															
			^{9}C	^{10}C	^{11}C	^{12}C ▨	^{13}C ▨	^{14}C	^{15}C 🟩	^{16}C	^{17}C	^{18}C	^{19}C 🟩	^{20}C		^{22}C 🟩															
			^{8}B 🟧		^{10}B ▨	^{11}B ▨	^{12}B	^{13}B	^{14}B	^{15}B		^{17}B 🟩		^{19}B 🟩																	
			^{7}Be		^{9}Be ▨	^{10}Be	^{11}Be 🟩	^{12}Be		^{14}Be 🟩																					
			^{6}Li ▨	^{7}Li ▨	^{8}Li	^{9}Li		^{11}Li 🟩																							
	^{3}He ▨	^{4}He ▨		^{6}He 🟩		^{8}He																									

Neutron dripline confirmed for $Z \leq 10$

▨ Stable nuclei
🟧 Proton-halo candidates
🟩 Neutron-halo candidates

^{22}Al: Lee *et al.*, PRL 125, 192503 (2020)
^{29}F: Bagchi *et al.*, PRL 124, 222504 (2020)
^{37}Mg: Kobayashi *et al.*, PRL 112, 242501 (2014)

Theoretical study of halo nuclei

➢ Few-body model	Zhukov *et al*., Phys. Rep. 231, 151 (1993)
➢ Shell model	Otsuka *et al*., PRL 70, 1385 (1993)
➢ Antisymmetrized molecular dynamics model	Horiuchi *et al*., ZPA 349, 279 (1994)
➢ Halo effective field theory	Bertulani *et al*., NPA 712, 37 (2002)
➢ Non-relativistic density functional theory	Terasaki *et al*., NPA 600, 371 (1996)
➢ Covariant density functional theory (CDFT)	Koepf *et al*., ZPA 340, 119 (1991)

➢ Advantages of the CDFT:

- ✓ Spin-orbit automatically included
- ✓ Lorentz covariance restricts parameters
- ✓ Pseudo-spin Symmetry
- ✓ Consistent treatment of time-odd fields
- ✓ Relativistic saturation mechanism
- ✓ …

Ring, PPNP 37, 193 (1996)
Vretenar *et al*., Phys. Rep. 409, 101 (2005)
Meng *et al*., PPNP 57, 470 (2006)
Niksic *et al*., PPNP 66, 519 (2011)
Meng and Zhou, JPG 42, 093101 (2015)
Liang *et al*., Phys. Rep. 570, 1 (2015)
Shen *et al*., PPNP 109, 103713 (2019)

Meng (Editor), *Relativistic Density Functional for Nuclear Structure* (World Scientific, 2016)

Spherical halo nuclei & Giant halos

- ✓ Based on the CDFT, a self-consistent description of the neutron halo in ^{11}Li is achieved by the relativistic continuum Hartree-Bogoliubov (RCHB) theory.

Meng and Ring, PRL 77, 3963 (1996)

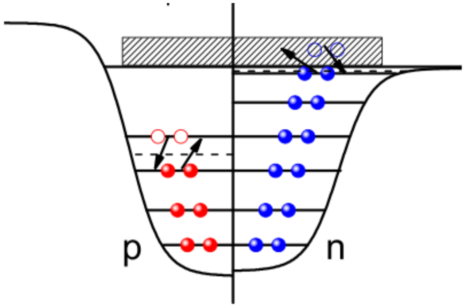

- ✓ Pairing correlations and continuum effects are very important for the description of halos.

Meng and Ring, PRL 77, 3963 (1996)
Meng *et al*., PPNP 57, 470 (2006)

- ✓ The RCHB theory also predicts giant halos in Zr isotopes.

Meng and Ring, PRL 80, 460 (1998)

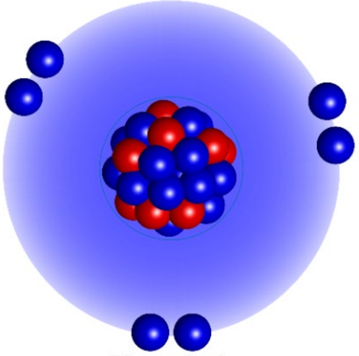
Giant-halo

- ✓ Later studies based on DFT and CDFT support the prediction of giant halos in Zr and Ca isotopes.

Meng, Toki, Zeng, Zhang, and Zhou, PRC 65, 041302(R) (2002)
Sandulescu, Geng, and Hillhouse, PRC 68, 054323 (2003)
Terasaki, Zhang, Zhou, Meng, PRC 74, 054318 (2006)
Grasso, Yoshida, Sandulescu, and Van Giai, PRC 74, 064317 (2006)

RCHB Mass Table

- ✓ Based on the RCHB theory, a nuclear mass table including continuum effects has been constructed.

Times Cited: 97 (Web of Science)

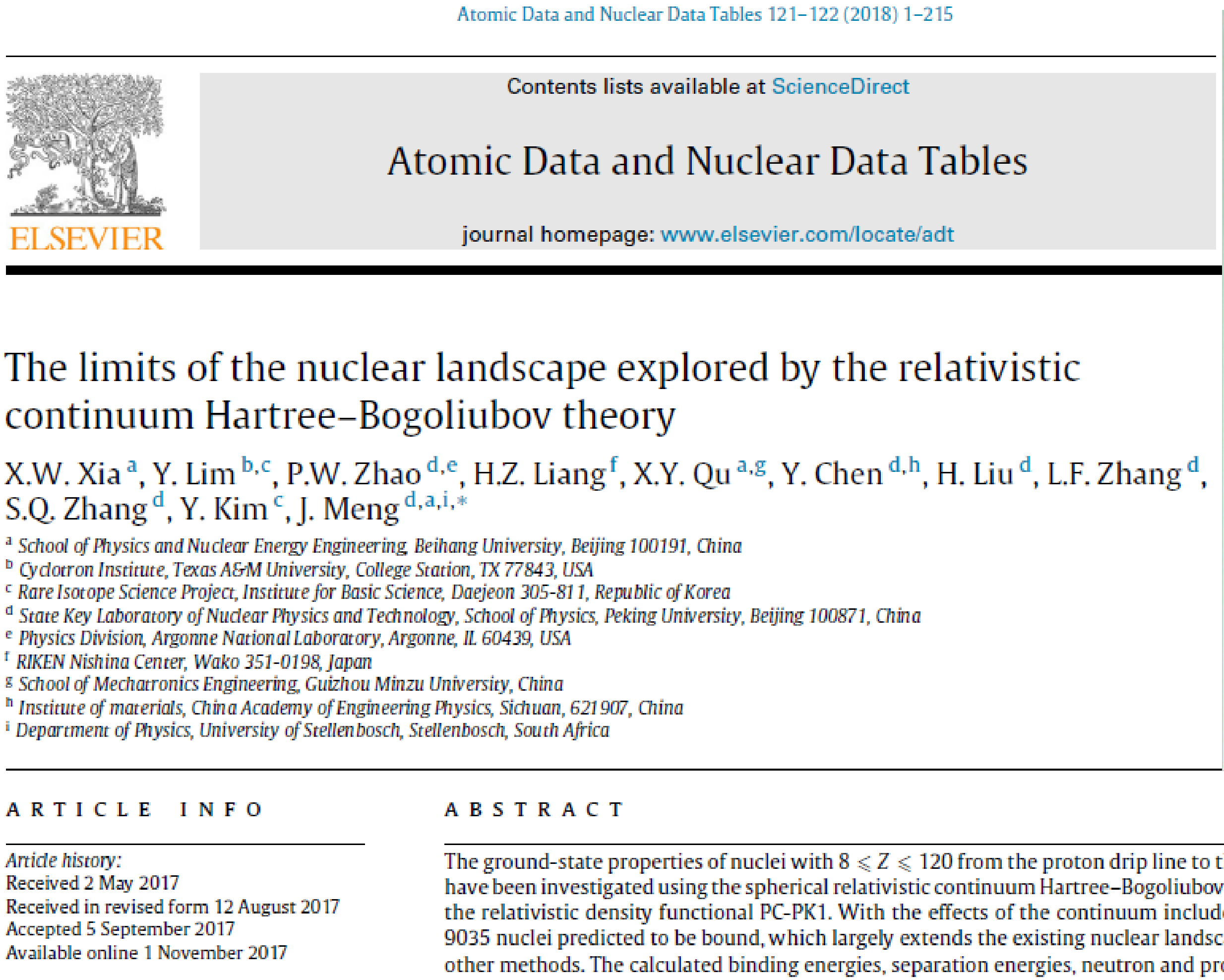

Atomic Data and Nuclear Data Tables 121–122 (2018) 1–215

Contents lists available at ScienceDirect

Atomic Data and Nuclear Data Tables

journal homepage: www.elsevier.com/locate/adt

ELSEVIER

The limits of the nuclear landscape explored by the relativistic continuum Hartree–Bogoliubov theory

X.W. Xia[a], Y. Lim[b,c], P.W. Zhao[d,e], H.Z. Liang[f], X.Y. Qu[a,g], Y. Chen[d,h], H. Liu[d], L.F. Zhang[d], S.Q. Zhang[d], Y. Kim[c], J. Meng[d,a,i,*]

[a] *School of Physics and Nuclear Energy Engineering, Beihang University, Beijing 100191, China*
[b] *Cyclotron Institute, Texas A&M University, College Station, TX 77843, USA*
[c] *Rare Isotope Science Project, Institute for Basic Science, Daejeon 305-811, Republic of Korea*
[d] *State Key Laboratory of Nuclear Physics and Technology, School of Physics, Peking University, Beijing 100871, China*
[e] *Physics Division, Argonne National Laboratory, Argonne, IL 60439, USA*
[f] *RIKEN Nishina Center, Wako 351-0198, Japan*
[g] *School of Mechatronics Engineering, Guizhou Minzu University, China*
[h] *Institute of materials, China Academy of Engineering Physics, Sichuan, 621907, China*
[i] *Department of Physics, University of Stellenbosch, Stellenbosch, South Africa*

ARTICLE INFO

Article history:
Received 2 May 2017
Received in revised form 12 August 2017
Accepted 5 September 2017
Available online 1 November 2017

ABSTRACT

The ground-state properties of nuclei with $8 \leqslant Z \leqslant 120$ from the proton drip line to the neutron drip line have been investigated using the spherical relativistic continuum Hartree–Bogoliubov (RCHB) theory with the relativistic density functional PC-PK1. With the effects of the continuum included, there are totally 9035 nuclei predicted to be bound, which largely extends the existing nuclear landscapes predicted with other methods. The calculated binding energies, separation energies, neutron and proton Fermi surfaces,

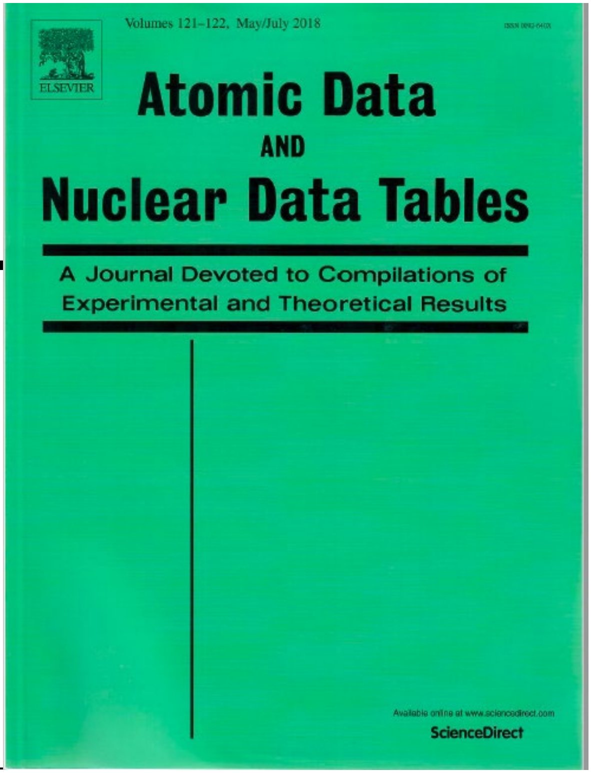

Volumes 121–122, May/July 2018

ELSEVIER

Atomic Data

AND

Nuclear Data Tables

A Journal Devoted to Compilations of Experimental and Theoretical Results

Available online at www.sciencedirect.com

ScienceDirect

Deformed halos

✓ There has been controversy over the existence of deformed halo nuclei.

Otsuka, Muta, Yokoyama, Fukunishi, and Suzuki, NPA 588, 113c (1995)
Misu, Nazarewicz, and Aberg, NPA 614, 44 (1997)
Tanihata, Hirata, and Toki, NPA 583, 769 (1995)
Nunes, NPA 757, 349 (2005)

✓ Considering axial deformation, pairing, and continuum effects, the deformed relativistic Hartree-Bogoliubov theory in continuum (DRHBc) predicts deformed halo nuclei.

Zhou, Meng, Ring, and Zhao, PRC 82, 011301(R) (2010)
Li, Meng, Ring, Zhao, and Zhou, PRC 85, 024312 (2012)

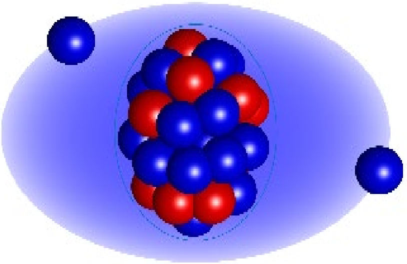

✓ Recently, several candidates of deformed halo nuclei have been suggested in experiment, such as ^{31}Ne and ^{37}Mg.

Nakamura *et al.*, PRL 112, 142501 (2014)
Kobayashi *et al.*, PRL 112, 242501 (2014)

✓ The DRHBc theory has been applied to study halo and other exotic phenomena.

Sun, Zhao, and Zhou, PLB 785, 530 (2018)
Zhang, Wang, and Zhang PRC 100, 034312 (2019)
Sun, Zhao, and Zhou, NPA 1003, 122011 (2020)

Sun, PRC 103, 054315 (2021)
Zhang *et al.*, PRC 104, L021301 (2021)
Pan *et al.*, PRC 104, 024331 (2021)
He *et al.*, CPC 45, 101001 (2021)

DRHBc Mass Table

✓ To construct a nuclear mass table including both deformation and continuum effects, the DRHBc Mass Table Collaboration was established.

Zhang *et al*. (DRHBc Mass Table Collaboration), PRC 102, 024314 (2020)

✓ Recently, the DRHBc mass table for even-even nuclei has been constructed, and it for odd nuclei is in progress.

Zhang *et al*. (DRHBc Mass Table Collaboration), ADNDT 144, 101488 (2022)
Pan *et al*. (DRHBc Mass Table Collaboration), arXiv:2205.01329

CDFT for nuclear masses

- **PC-PK1 + DRHBc, 2583 even-even nuclei with $8 \le Z \le 120$, first mass table including both deformation and continuum, $\sigma = 1.5$ MeV**

K. Y. Zhang *et al*. (DRHBc Mass Table Collaboration), Nuclear mass table in deformed relativistic Hartree–Bogoliubov theory in continuum, I: Even–even nuclei, **At. Data Nucl. Data Tables** 144, 101488 (2022)

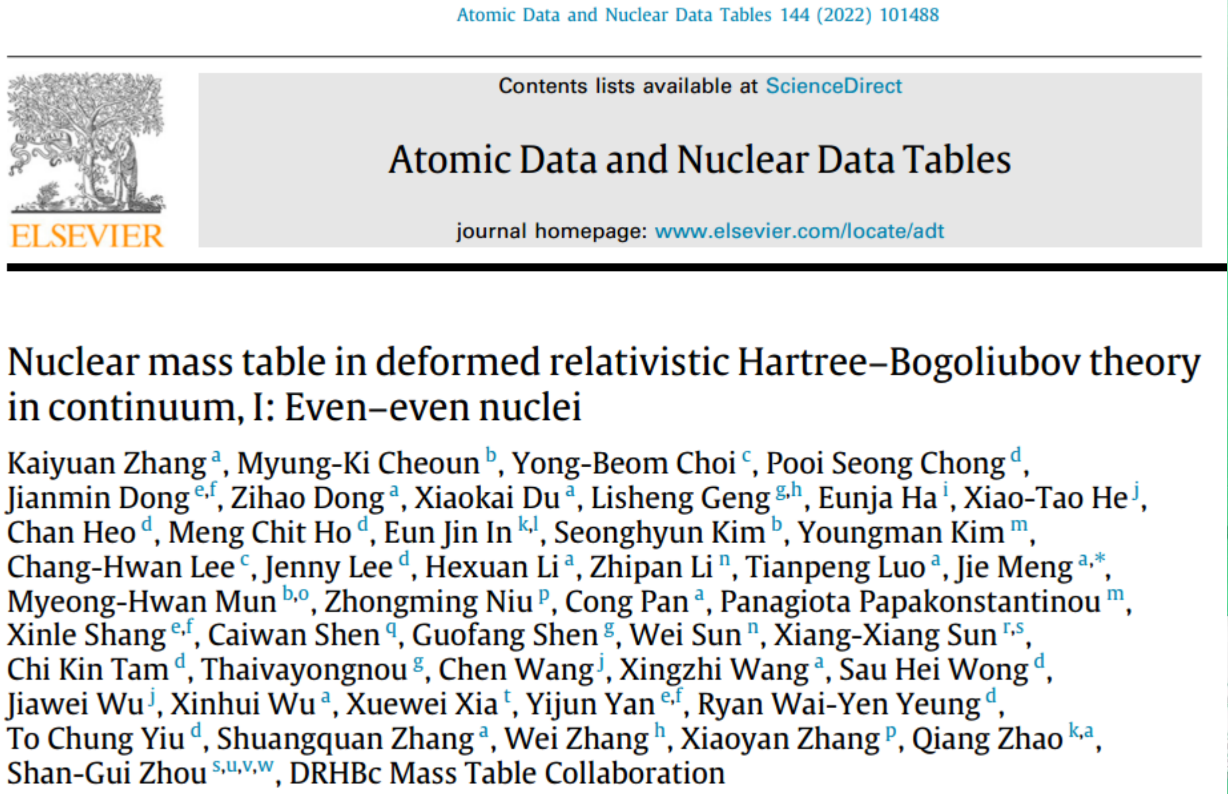

Atomic Data and Nuclear Data Tables 144 (2022) 101488

Contents lists available at ScienceDirect

Atomic Data and Nuclear Data Tables

journal homepage: www.elsevier.com/locate/adt

Nuclear mass table in deformed relativistic Hartree–Bogoliubov theory in continuum, I: Even–even nuclei

Kaiyuan Zhang[a], Myung-Ki Cheoun[b], Yong-Beom Choi[c], Pooi Seong Chong[d],
Jianmin Dong[e,f], Zihao Dong[a], Xiaokai Du[a], Lisheng Geng[g,h], Eunja Ha[i], Xiao-Tao He[j],
Chan Heo[d], Meng Chit Ho[d], Eun Jin In[k,l], Seonghyun Kim[b], Youngman Kim[m],
Chang-Hwan Lee[c], Jenny Lee[d], Hexuan Li[a], Zhipan Li[n], Tianpeng Luo[a], Jie Meng[a,*],
Myeong-Hwan Mun[b,o], Zhongming Niu[p], Cong Pan[a], Panagiota Papakonstantinou[m],
Xinle Shang[e,f], Caiwan Shen[q], Guofang Shen[g], Wei Sun[n], Xiang-Xiang Sun[r,s],
Chi Kin Tam[d], Thaivayongnou[g], Chen Wang[j], Xingzhi Wang[a], Sau Hei Wong[d],
Jiawei Wu[j], Xinhui Wu[a], Xuewei Xia[t], Yijun Yan[e,f], Ryan Wai-Yen Yeung[d],
To Chung Yiu[d], Shuangquan Zhang[a], Wei Zhang[h], Xiaoyan Zhang[p], Qiang Zhao[k,a],
Shan-Gui Zhou[s,u,v,w], DRHBc Mass Table Collaboration

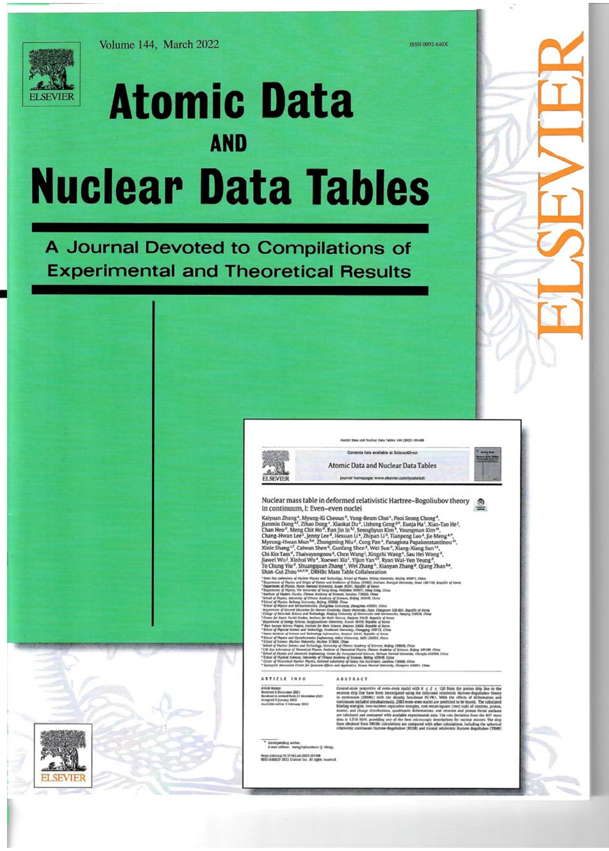

Volume 144, March 2022

Atomic Data
AND
Nuclear Data Tables

A Journal Devoted to Compilations of Experimental and Theoretical Results

ELSEVIER

Triaxially deformed halo nucleus?

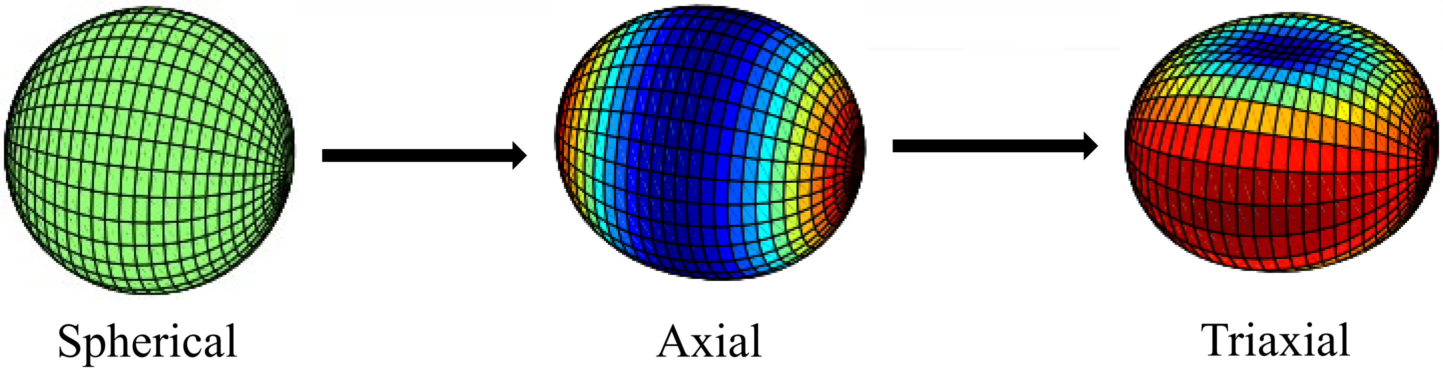

- ✓ Triaxial deformation plays a crucial role in nuclear chirality, wobbling motion, and fission.

Frauendorf and Meng, Nucl. Phys. A 617, 131 (1997)
Bohr and Mottelson, *Nuclear Structure* (1975)
Lu, Zhao, and Zhou, PRC 85, 011301(R) (2012)

- ✓ A study based on triaxial Woods-Saxon potential suggests that the triaxial deformation might extend the region of halo nuclei.

Uzawa, Hagino, and Yoshida, PRC 104, L011303 (2021)

Recently, a triaxial relativistic Hartree-Bogoliubov theory in continuum (TRHBc), which considers triaxial deformation, pairing, and continuum effects, is developed to search for triaxially deformed halo nuclei.

Zhang, Ph.D. thesis, Peking University (2022)

Contents

◆ Introduction

◆ Theoretical framework

◆ Results and discussion

◆ Summary

CDFT: Point-coupling model

Meng (Editor), *Relativistic Density Functional for Nuclear Structure* (2016)

✓ The starting point is a effective Lagrangian density,

$$\mathcal{L} = \mathcal{L}^{\rm free} + \mathcal{L}^{\rm 4f} + \mathcal{L}^{\rm der} + \mathcal{L}^{\rm hot} + \mathcal{L}^{\rm em},$$

$$\mathcal{L}^{\rm free} = \bar\psi(i\gamma_\mu\partial^\mu - M)\psi.$$

$$\begin{aligned}\mathcal{L}^{\rm 4f} = &-\frac{1}{2}\alpha_S(\bar\psi\psi)(\bar\psi\psi) - \frac{1}{2}\alpha_V(\bar\psi\gamma_\mu\psi)(\bar\psi\gamma^\mu\psi)\\ &-\frac{1}{2}\alpha_{TS}(\bar\psi\vec\tau\psi)(\bar\psi\vec\tau\psi) - \frac{1}{2}\alpha_{TV}(\bar\psi\vec\tau\gamma_\mu\psi)(\bar\psi\vec\tau\gamma^\mu\psi).\end{aligned}$$

$$\begin{aligned}\mathcal{L}^{\rm der} = &-\frac{1}{2}\delta_S\partial_\nu(\bar\psi\psi)\partial^\nu(\bar\psi\psi) - \frac{1}{2}\delta_V\partial_\nu(\bar\psi\gamma_\mu\psi)\partial^\nu(\bar\psi\gamma^\mu\psi)\\ &-\frac{1}{2}\delta_{TS}\partial_\nu(\bar\psi\vec\tau\psi)\partial^\nu(\bar\psi\vec\tau\psi) - \frac{1}{2}\delta_{TV}\partial_\nu(\bar\psi\vec\tau\gamma_\mu\psi)\partial^\nu(\bar\psi\vec\tau\gamma^\mu\psi)\end{aligned}$$

$$\mathcal{L}^{\rm hot} = -\frac{1}{3}\beta_S(\bar\psi\psi)^3 - \frac{1}{4}\gamma_S(\bar\psi\psi)^4 - \frac{1}{4}\gamma_V[(\bar\psi\gamma_\mu\psi)(\bar\psi\gamma^\mu\psi)]^2$$

$$\mathcal{L}^{\rm em} = -\frac{1}{4}F^{\mu\nu}F_{\mu\nu} - e\bar\psi\gamma^\mu\frac{1-\tau_3}{2}A_\mu\psi$$

M： nucleon mass

$\alpha_S, \alpha_V, \alpha_{TV}, \delta_S, \delta_V, \delta_{TV}, \beta_S, \gamma_S, \gamma_V$： coupling constants

RHB equations

- ✓ Relativistic Hartree-Bogoliubov (RHB) equations for nucleons read

$$\begin{pmatrix} \hat{h}_D-\lambda & \hat{\Delta} \\ -\hat{\Delta}^* & -\hat{h}_D^*+\lambda \end{pmatrix}\begin{pmatrix} U_k \\ V_k \end{pmatrix} = E_k \begin{pmatrix} U_k \\ V_k \end{pmatrix}.$$

- λ is the Fermi energy, E_k is the quasi-particle energy, and $(U_k, V_k)^T$ is the quasi-particle wave function.

- The Dirac Hamiltonian $h_D(\boldsymbol{r}) = \boldsymbol{\alpha}\cdot[\boldsymbol{p}-\boldsymbol{V}(\boldsymbol{r})] + V^0(\boldsymbol{r}) + \beta[M+S(\boldsymbol{r})]$

$$\begin{aligned} S(\boldsymbol{r}) =& \alpha_S\rho_S + \beta_S\rho_S^2 + \gamma_S\rho_S^3 + \delta_S\Delta\rho_S, \\ V^\mu(\boldsymbol{r}) =& \alpha_V j^\mu + \gamma_V(j_\mu j^\mu)j^\mu + \delta_V\Delta j^\mu + eA^\mu \\ &+ \alpha_{TV} j_3^\mu + \delta_{TV}\Delta j_3^\mu. \end{aligned}$$

$$\begin{aligned} \rho_S(\boldsymbol{r}) &= \sum_k \bar{V}_k(\boldsymbol{r})V_k(\boldsymbol{r}), \\ j^\mu(\boldsymbol{r}) &= \sum_k \bar{V}_k(\boldsymbol{r})\gamma^\mu V_k(\boldsymbol{r}), \\ j_3^\mu(\boldsymbol{r}) &= \sum_k \bar{V}_k(\boldsymbol{r})\gamma^\mu\tau_3 V_k(\boldsymbol{r}), \\ j_c^\mu(\boldsymbol{r}) &= \sum_k \bar{V}_k(\boldsymbol{r})\gamma^\mu\frac{1-\tau_3}{2}V_k(\boldsymbol{r}). \end{aligned}$$

- The pairing potential $\Delta(\boldsymbol{r}_1,\boldsymbol{r}_2) = V^{pp}(\boldsymbol{r}_1,\boldsymbol{r}_2)\kappa(\boldsymbol{r}_1,\boldsymbol{r}_2)$

Spherical harmonic expansion

✓ To include triaxial deformation, densities and potentials are expanded in terms of spherical harmonic functions,

$$f(\boldsymbol{r}) = \sum_{\lambda\mu} f_{\lambda\mu}(r) Y_{\lambda\mu}(\theta, \varphi)$$

✓ According to spatial reflection symmetry and reflection symmetries with respect to *xy*, *xz*, and *yz* plane,

$$\hat{P} f(\boldsymbol{r}) = \sum_{\lambda\mu} f_{\lambda\mu}(r) Y_{\lambda\mu}(\pi - \theta, \pi + \varphi) = \sum_{\lambda\mu} f_{\lambda\mu}(r) (-1)^{\lambda} Y_{\lambda\mu}(\theta, \varphi)$$

$$\hat{P}_z f(\boldsymbol{r}) = \sum_{\lambda\mu} f_{\lambda\mu}(r) Y_{\lambda\mu}(\pi - \theta, \varphi) = \sum_{\lambda\mu} f_{\lambda\mu}(r) (-1)^{\lambda+\mu} Y_{\lambda\mu}(\theta, \varphi)$$

$$\hat{P}_x f(\boldsymbol{r}) = \sum_{\lambda\mu} f_{\lambda\mu}(r) Y_{\lambda\mu}(\theta, \pi - \varphi) = \sum_{\lambda\mu} f_{\lambda\mu}(r) Y_{\lambda-\mu}(\theta, \varphi)$$

λ, μ are restricted to be even numbers, and $-\mu$ component is equal to μ component.

Dirac Woods-Saxon basis

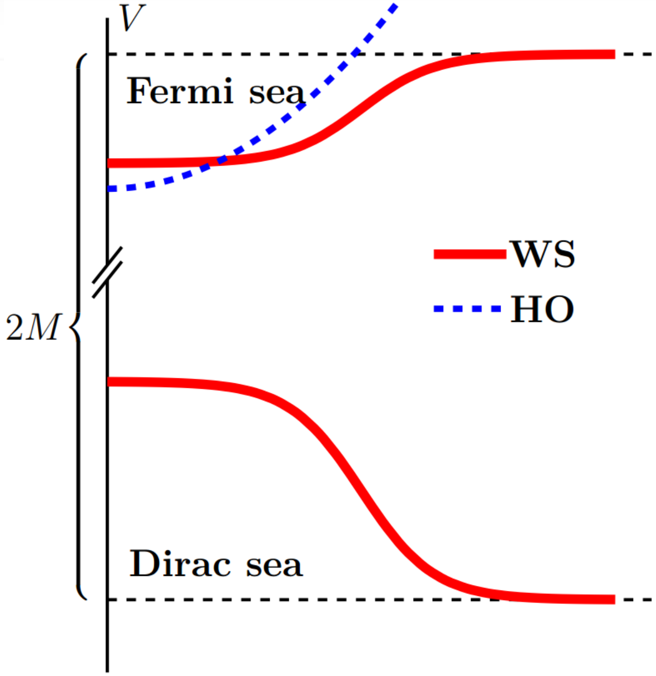

- ✓ In the TRHBc theory, the RHB equations are solved in a Dirac Woods-Saxon (DWS) basis, whose wave function has a more realistic behavior at large *r* compared with the HO basis.

- ✓ The DWS basis is obtained by solving a Dirac equation containing the spherical Woods-Saxon potential. Because the basis function itself is a Dirac spinor, there is no need to expand upper and lower components separately.

Zhou, Meng, and Ring, PRC 68, 034323 (2003)

$$\hat{h}_0|\varphi_{n\kappa m}\rangle = \epsilon_{n\kappa}|\varphi_{n\kappa m}\rangle, \quad \varphi_{n\kappa m}(\boldsymbol{r}\sigma) = \frac{1}{r}\begin{pmatrix} iG_{n\kappa}(r)Y^{l}_{jm}(\Omega\sigma) \\ -F_{n\kappa}(r)Y^{\tilde{l}}_{jm}(\Omega\sigma) \end{pmatrix}$$

Contents

- ◆ Introduction
- ◆ Theoretical framework
- ◆ **Results and discussion**
- ◆ Summary

Numerical details

✓ Density functional： PC-PK1, NL3*, NLSH, PK1

✓ Pairing interaction： Density-dependent zero-range pairing force

✓ Box size： $R_{\text{box}} = 20$ fm

✓ Mesh size： $\Delta r = 0.1$ fm

✓ Energy cutoff： $E_{\text{cut}} = 300$ MeV

✓ Angular momentum cutoff： $J_{\max} = 19/2\ \hbar$

✓ Pairing strength： $V_0 = -342.5$ MeV fm^3

Xia *et al*., ADNDT 121–122, 1 (2018)

✓ Spherical harmonic expansion order： $\lambda_{\max} = 6$

Zhang *et al*. (DRHBc Mass Table Collaboration), PRC 102, 024314 (2020)
Pan, Zhang, and Zhang, IJMPE 28, 1950082 (2019)

Deformation of Al isotopes

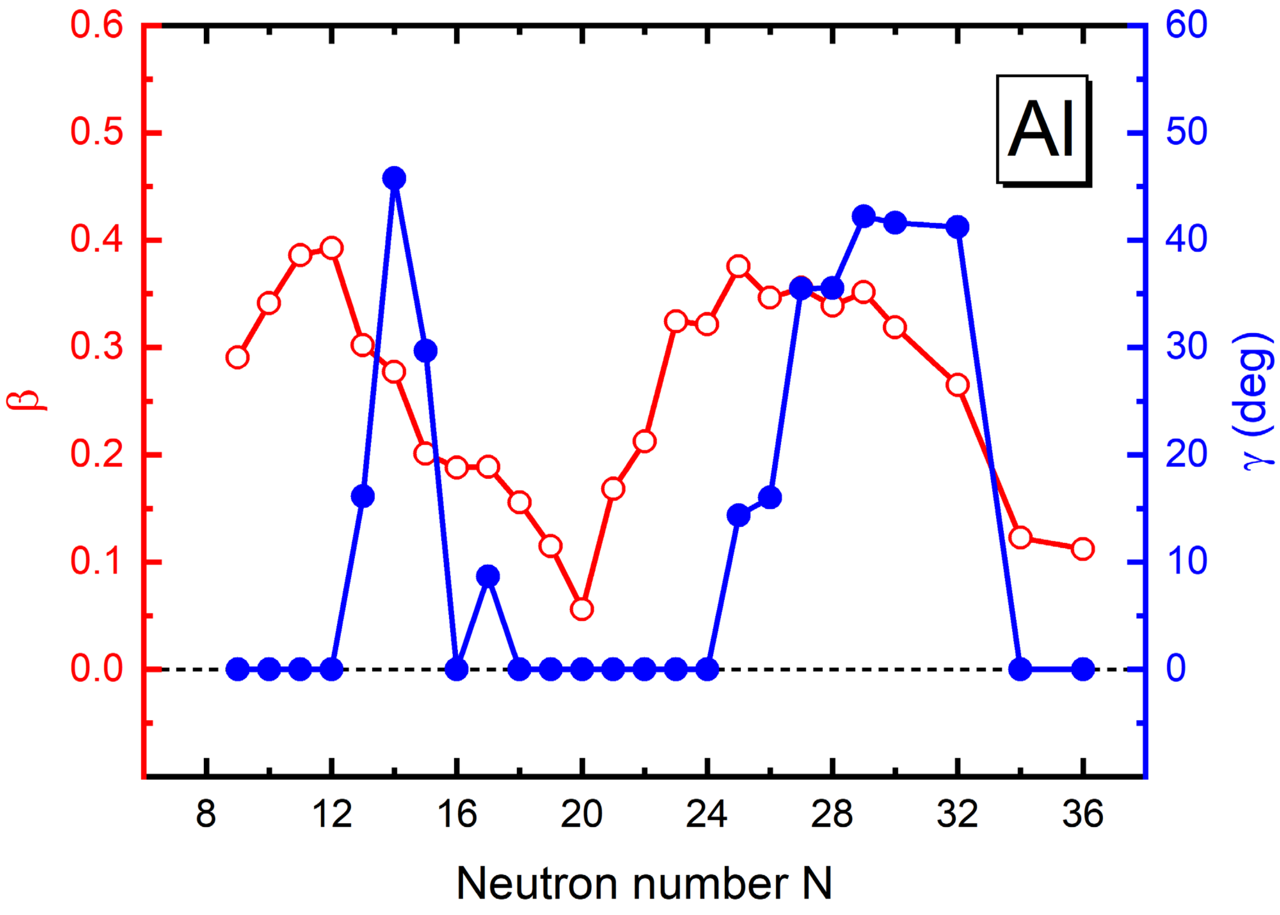

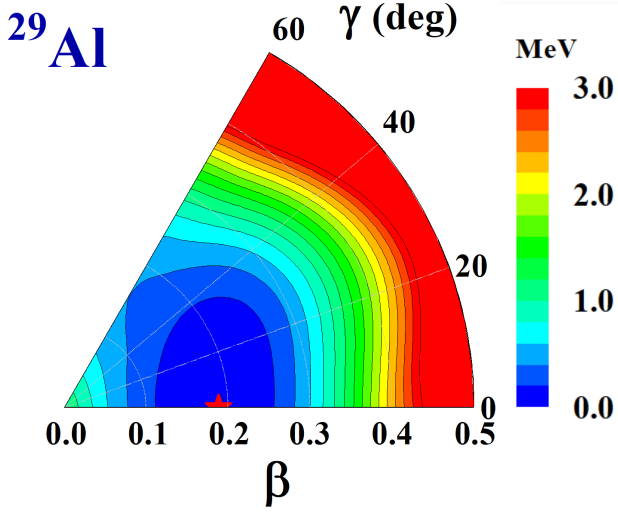

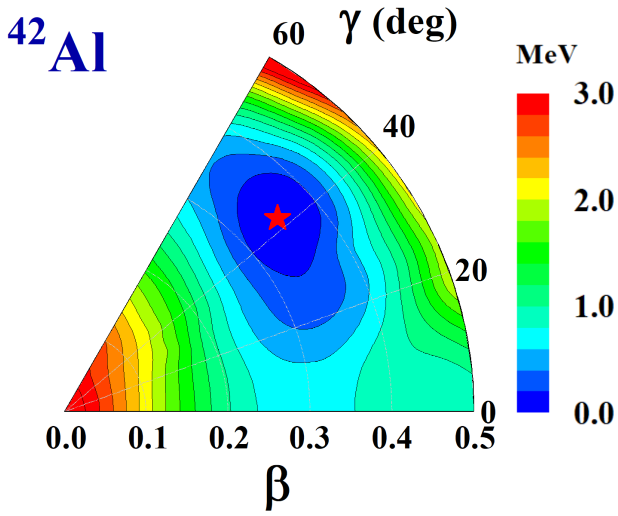

✓ Light neutron-rich nuclei are calculated, and several Al isotopes are found to be triaxially deformed.

Observables

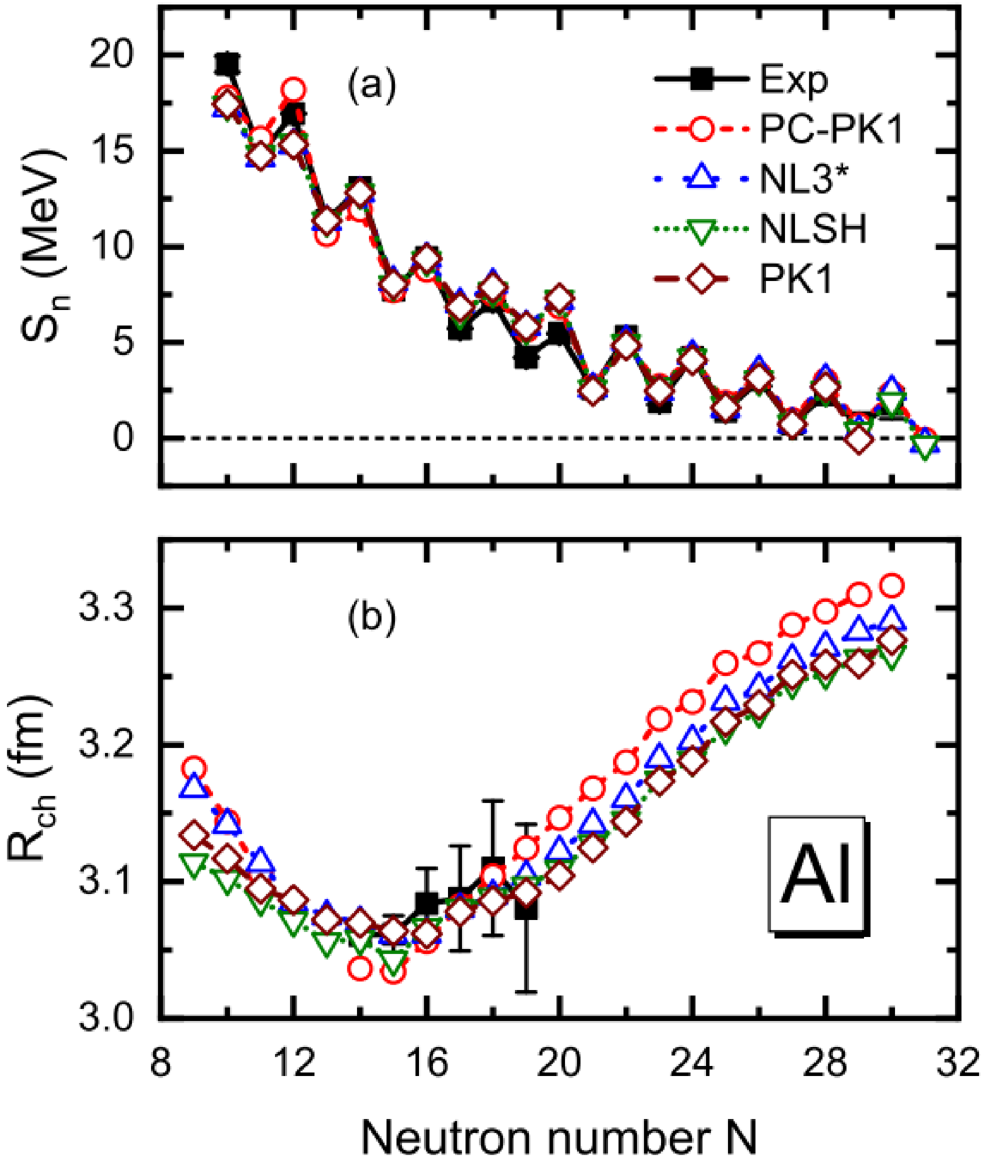

S_n data taken from CPC 45, 030003 (2021)
[Experimental values for $11 \leq N \leq 25$]

R_{ch} data taken from PRC 103, 014318 (2021)

✓ AME2020 data and experimental charge radii are reproduced well.

✓ ^{42}Al is triaxially deformed, and it has a small $S_n = 0.67(64)$ MeV.

Increase of neutron radii

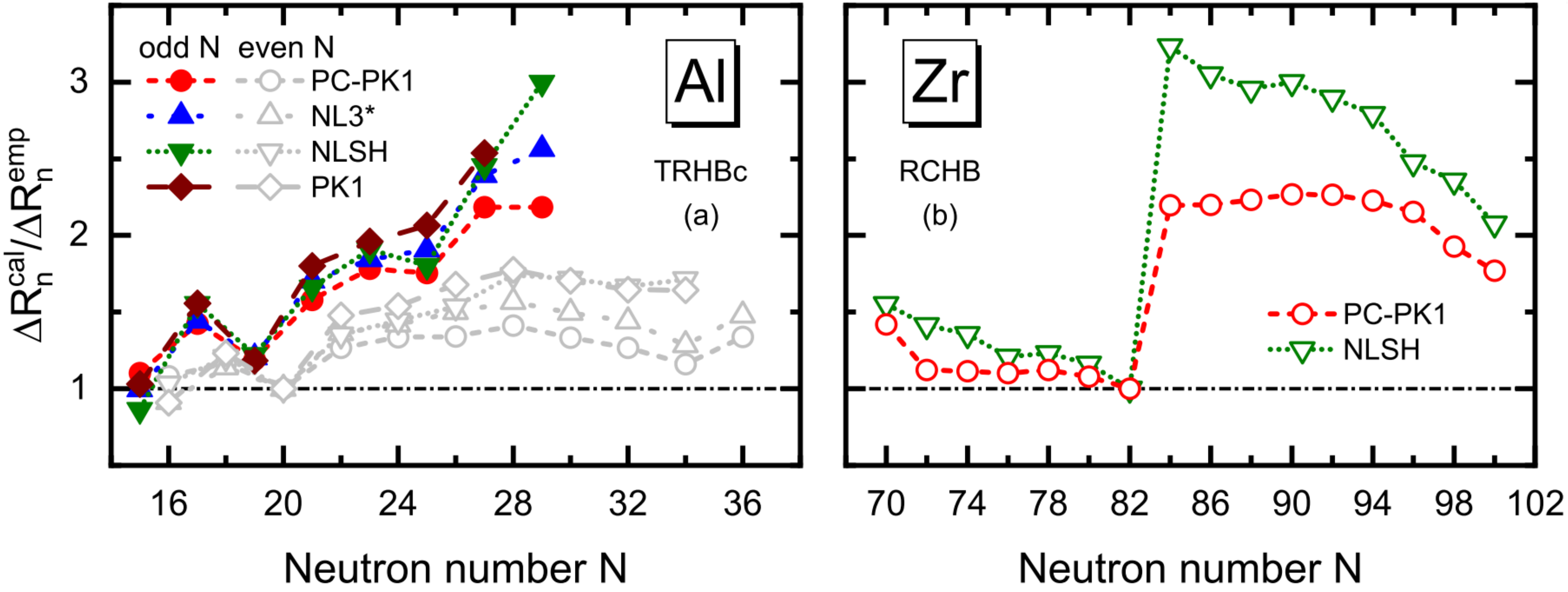

$$R_n^{\text{emp}} = r_0 N^{1/3}$$

RCHB + PC-PK1: ADNDT 121–122, 1 (2018)
RCHB + NLSH: PRL 80, 460 (1998)

✓ The ratio of TRHBc calculated neutron radius increment to that from empirical formula increases significantly at ^{40,42}Al, which is similar to the increase in giant halo Zr isotopes.

Neutron levels, radii, and contribution

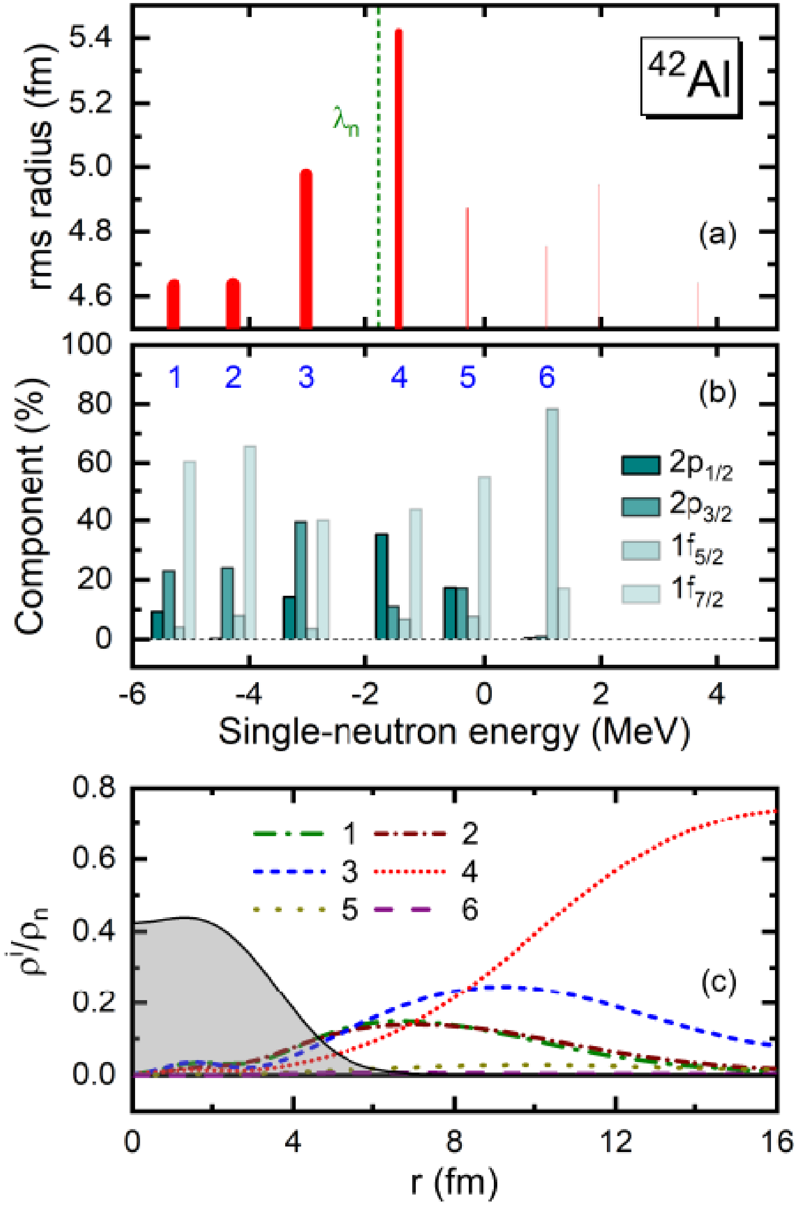

- ✓ Weakly bound level 4 occupied by the valance neutron has a remarkably large rms radius.
- ✓ Level 4 has considerable *2p* components (≥ 45%).
- ✓ Level 4 contributes dominantly to the total neutron density in the region far from center.

Density in different planes

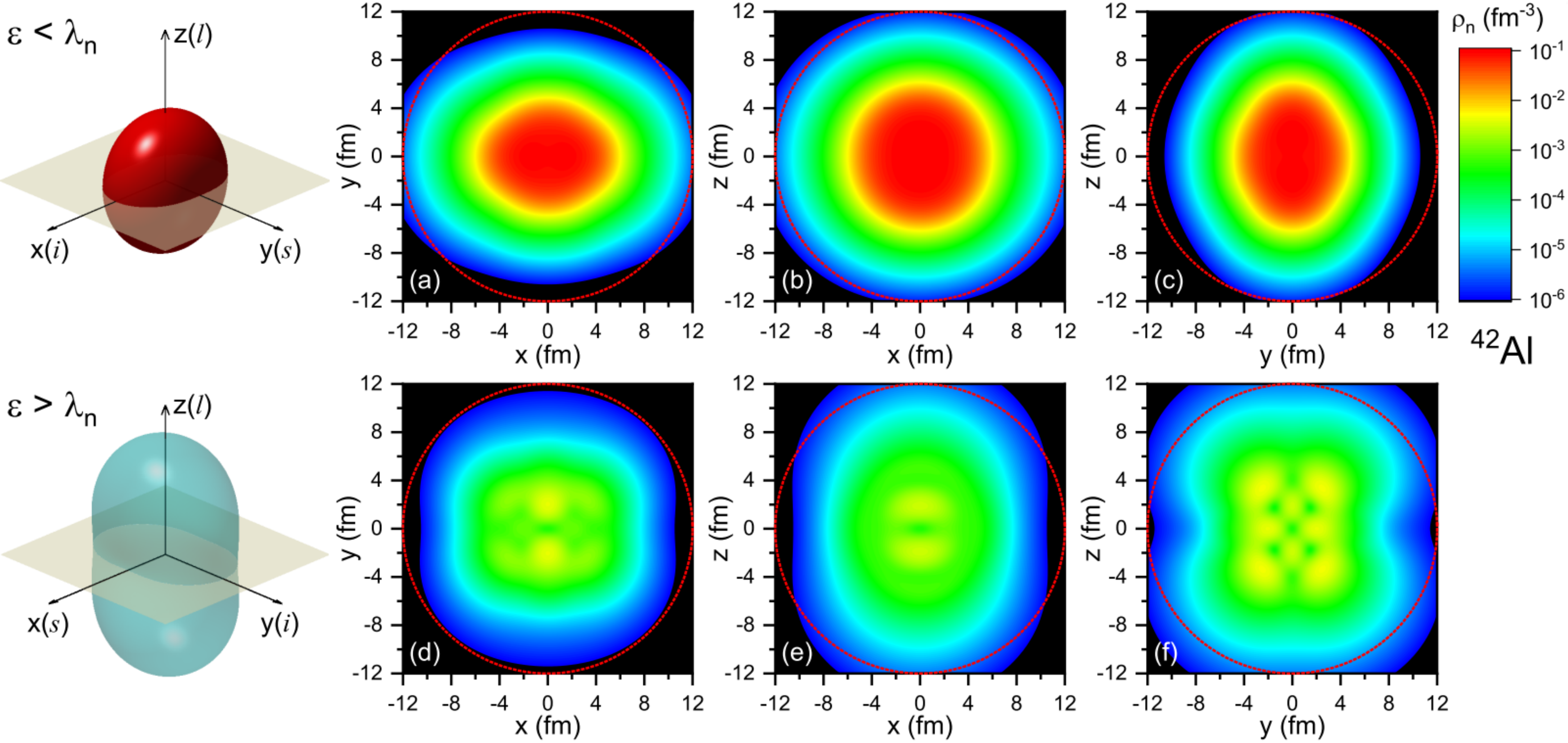

- ✓ Core: $r = 3.85$ fm, $\beta = 0.38$, $\gamma = 50°$, $z > x > y$
- ✓ Halo: $r = 5.26$ fm, $\beta = 0.79$, $\gamma = -23°$, $z > y > x$

Contents

- ◆ Introduction
- ◆ Theoretical framework
- ◆ Results and discussion
- ◆ Summary

Summary

- ✓ RCHB and DRHBc theories based on the CDFT have been successful for spherical and deformed halo nuclei.

- ✓ Triaxial relativistic Hartree-Bogoliubov theory in continuum (TRHBc) is developed to explore triaxially deformed halo nuclei.

- ✓ TRHBc theory reproduces available experimental data for Al isotopes. ^{42}Al has triaxially deformed ground state, small S_n, and suddenly increased neutron radius.

- ✓ The orbital occupied by the valance odd neutron of ^{42}Al has a significantly large radius, due to its weak binding and considerable 2*p* components, and it contributes dominantly to neutron density at large *r*.

- ✓ Decomposed neutron densities suggest that ^{42}Al is a triaxially deformed halo nucleus with a triaxial shape decoupling between the core and the halo.

Thank you for your attention!